AMAS Workshop on Nondestructive Testing of Materials
NTM'03 – (pp.35–51) – Warsaw, May 19-21, 2003.

Ultrasonic phased arrays

T. STĘPIŃSKI

Signals and Systems
Uppsala University, Sweden
ts@signal.uu.se

This paper is intended as an introduction to phased arrays and their applications to NDE. Fundamentals required for proper understanding phased array operation are presented in the first part. Based on time-domain beamforming principle the concepts of beam steering, beam focusing, spatial aliasing, and resolution are presented. Issues related to beamformer hardware design are shortly discussed and some practical applications of phased arrays in NDE are presented.

1. Introduction

Nondestructive evaluation (NDE) is an essential inspection method for ensuring the safe and long-term operation of plants. Ultrasonic testing (UT) is widely used for the inspection of many products and for the assessment of different structures. The UT method produces satisfactory result when applied for detecting and sizing defects in the structures characterized by a relatively simple geometry and free access to the surfaces. However, the application of the conventional UT to structures and parts with complex geometry is limited by the possibility of scanning the ultrasonic probe. In many cases mechanical scanning of the ultrasonic probes considerably increases inspection time and also as a consequence the inspection cost.

Recent developments of ultrasonic phased array hardware for NDE has enabled a wide use of this technology in industrial applications [5, 6, 7]. Beam patterns of phased arrays can be controlled electronically, in other words, electronic beam steering and focusing is possible without moving the array or changing the conventional ultrasonic probes. This creates a considerable flexibility that accelerates inspecting parts with complex geometry and facilitates the use of UT in many practical applications.

This paper gives a short review of beamforming fundamentals required for proper understanding phased array operation. The theory is illustrated by plots of simulated results showing the influence of different array param-

eters essential for the beamforming. The theoretical part is followed by the presentation of some practical applications of phased arrays to NDE.

2. Beamforming

A beam is formed using an ultrasonic array by steering its beam pattern in a desired direction, thus enhancing this particular spatial direction and attenuating the other directions. An ultrasonic image of the region of interest defined in terms of range (time) and bearing (direction) can be then composed from different beams. Beamforming that is normally applied both in the transmission and reception modes, is the process of combining the outputs of a phased array in such a way as to achieve spatial selectivity. Modern beamforming process is typically implemented using digital processors and associated electronic hardware, resulting in low maintenance costs and high scan rates.

Beamforming in the reception mode is a method of observing signals from a desired direction while attenuating the response of the array to signals from other directions. Beamforming can permit a multi-dimensional view of a medium using an appropriate array of sensors, and thus have many applications, including medicine, astronomy and military devices [2, 4]. Below, we will present an introduction to time-domain beamforming using a simple 2-dimensional case as an illustration.

Let us consider the reception mode where the reflections from the objects located at array's far field are received, this means that the distance from the array to the objects is large enough, so that the wave fronts reaching the targets are parallel to the array.

Further, we assume that the received waves take the form of a sinusoidal modulated signal with spatial information inscribed by the reflections from

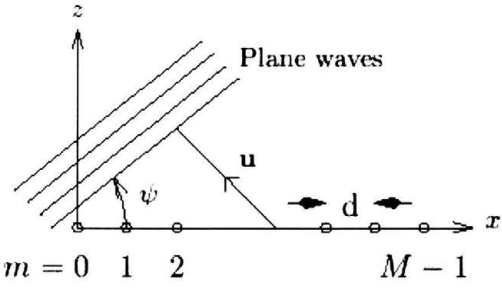

FIGURE 1. Linear array consisting of M elements separated by a distance d along x-axis receives plane waves incident with an angle ψ.

the objects to be detected. The signal propagates through the medium with speed c as a plane wave of angular frequency ω and the associated wave number $k = \omega/c$. Denote the position of the individual element m as $\mathbf{r}_m$and define the orientation of the plane wave using the directional (column) vector $\mathbf{u}$ (see Fig. 1). Then the signal received at m-th sensor is

$$x_m(t) = e^{j(\omega t + k\,\mathbf{r}_m^T \cdot \mathbf{u})} = x(t)\, e^{jkr_m} \quad \text{for} \quad m = 0, \ldots, M-1,$$

where $x(t) = e^{j(\omega t)}$, and $r_m = \mathbf{r}_m^T \cdot \mathbf{u}$ is the projection of $\mathbf{r}_m$ on $\mathbf{u}$ which defines an additional relative distance that a wave coming from the direction $\mathbf{u}$ propagates to reach a sensor located at $\mathbf{r}_m$.

If the outputs of M sensors in the array are summed the array will act as a spatial filter that enhances the direction normal to the array. In such a case the array output $y(t)$ will be described by a *general beamforming equation*, that is

$$y(t) = \mathbf{a} \cdot \mathbf{X}(t) = x(t)\, \mathbf{a} \cdot e^{j\mathbf{k}\,\mathbf{r}}, \tag{2.1}$$

where $\mathbf{a}$ denotes a window function, $\mathbf{X}$(t) denotes all sensor outputs, and $\mathbf{r}$ denotes respective phase delays of individual sensors, such that

$$\begin{aligned} \mathbf{a} &= [a_0 \ \ldots \ a_{M-1}], \\ \mathbf{X}(t) &= [x_0(t) \ \ldots \ x_{M-1}(t)]^T = x(t)\, e^{j\mathbf{k}\,\mathbf{r}}, \\ \mathbf{r} &= [r_0 \ \ldots \ r_{M-1}]^T. \end{aligned}$$

The window function $\mathbf{a}$ defines apodization, i.e., gains applied to individual elements of the array in order to modify its beam pattern. The main function of the window function is suppressing side lobes that appear on both sides of the main lobe. This can be observed in Fig. 2 where the beam patterns obtained for a rectangular window (no apodization) and for the Hamming window[1)] can be compared. The beam patterns presented in Fig. 2 are calculated for the 32-element array with point-like elements spaced with $d = 0.74\,\text{mm} < \lambda/2$ for a continuous wave (CW) with frequency 1 MHz in water. This array, which will be referred to as A32EL will be used below as an example illustrating the presented theory. From Fig. 2, it can be seen that apodization reduces side lobe level at the price of decreased resolution (broader main lobe).

3. Beam steering

Steering or spatial filtering in a particular direction, $\mathbf{u}_0$, is achieved by coherent summation of the array outputs, $X(t)$, for this direction. This is

[1)] Hamming window is a cosine type apodization using function $0.54 - 0.46\cos(2\pi m/M)$.

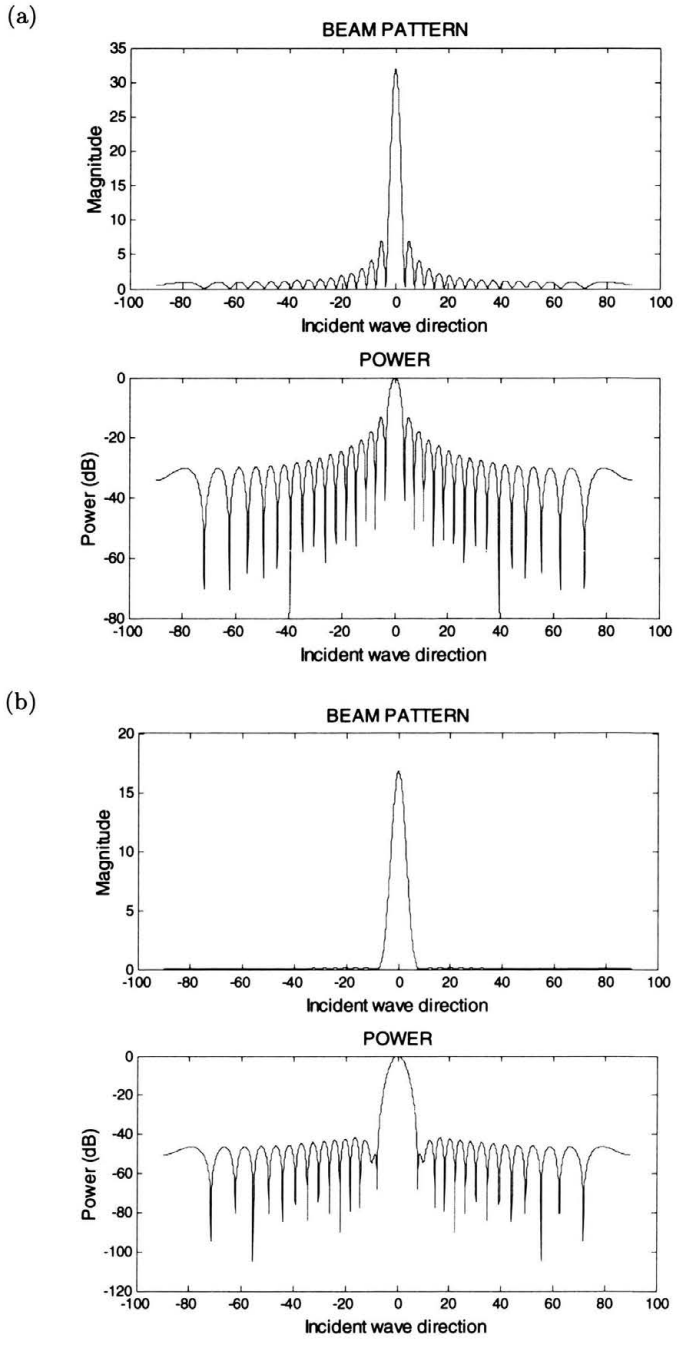

FIGURE 2. Theoretical beam patterns in far field for 32-element arrays in water without apodization (a) and with apodization using Hamming window (b). Frequency 1 MHz, element spacing 0.74 mm, $\lambda = 1.5$ mm.

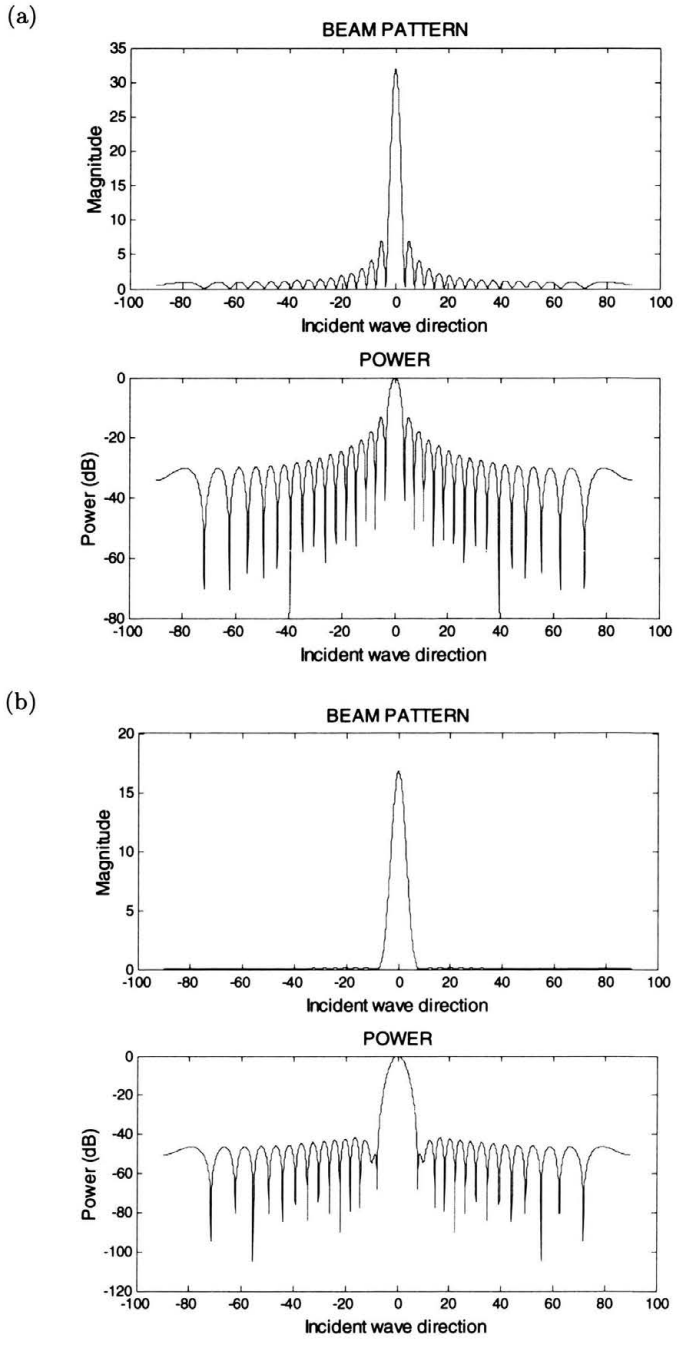

FIGURE 2. Theoretical beam patterns in far field for 32-element arrays in water without apodization (a) and with apodization using Hamming window (b). Frequency 1 MHz, element spacing 0.74 mm, $\lambda = 1.5$ mm.

achieved by introducing time delays varying linearly with element number so that a planar wave is sent in the desired direction. This leads to the general beamforming equation

$$y(t, \mathbf{u}_0) = x(t)\, \mathbf{a} \cdot e^{jk(\mathbf{r}-\mathbf{r}_0)} = x(t)\, b(\omega, \mathbf{u}_0), \tag{3.1}$$

where the *beam pattern*, $b(\omega, \mathbf{u}_0)$, is given by

$$b(\omega, \mathbf{u}_0) = \mathbf{a} \cdot e^{jk(\mathbf{r}-\mathbf{r}_0)}. \tag{3.2}$$

For a linear array consisting of M elements the beamforming equation takes the form

$$b(t, \psi_0) = \mathbf{a} \cdot e^{jkd\mathbf{m}\sin\psi_0}, \tag{3.3}$$

where $\mathbf{m} = [0\ 1\ \ldots\ (M-1)]^T$, and ψ_0 the desired bearing (steering direction).

Beam steering is illustrated by the beam patterns presented in Fig. 3 obtained for a 32-element array without apodization and with apodization using Bartlett (triangular) window. The simulation was performed for CW with frequency 1 MHz in water for the array A32EL. From Fig. 3, it can be seen that apodization is essential for the steered beams since it substantially reduces the side lobe level.

4. Beam focusing

Focusing at a particular point at a distance f from the array is achieved by coherent summation of sensor outputs, $X(t)$, so that beams from all elements meet in phase in this point. This is achieved by introducing time delays compensating the elements distance to this point so that a cylindrical wave is sent in the desired direction. For focusing a linear array consisting of M elements in far field the beamforming equation becomes

$$b(t, \psi_0) = \mathbf{a} \cdot e^{jkd\mathbf{p}_m}, \quad \text{where} \quad \mathbf{p}_m = \frac{d}{2f}\left[0\ \ldots\ (M-1)^2\right]. \tag{4.1}$$

Simultaneous beamforming and focusing consists in superposing both time delays as it is illustrated in Fig. 4. Radiation emitted by the array A32EL focused at a distance of 30 mm for 1 MHz CW in water is shown in Fig. 5. Cross sections of the radiated field are shown in Figs. 5 and 6. From Figs. 6 and 7, it can be seen that the array's beam power has a well pronounced maximum at the focal distance in the direction 0°.

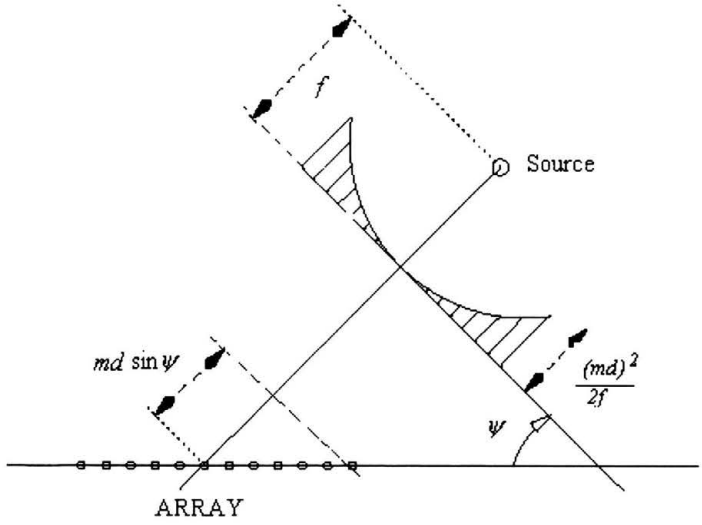

FIGURE 4. Steering and focusing of linear array.

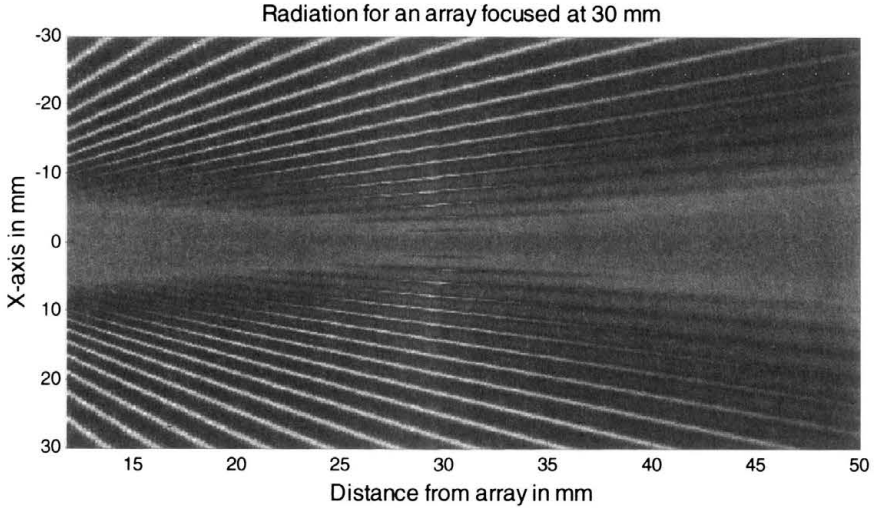

FIGURE 5. Radiation from the 32-element array in water without apodization. Frequency 1 MHz, element spacing 0.74 mm, $\lambda = 1.5$ mm.

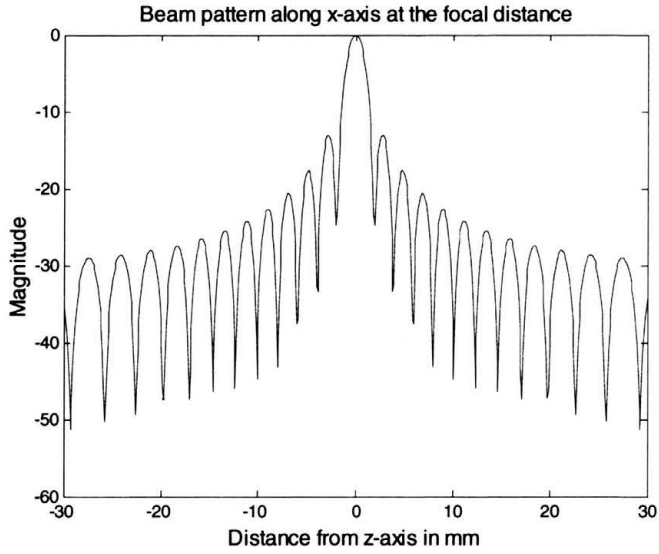

FIGURE 6. Radiation pattern from the array shown in Fig. 5 at focal point.

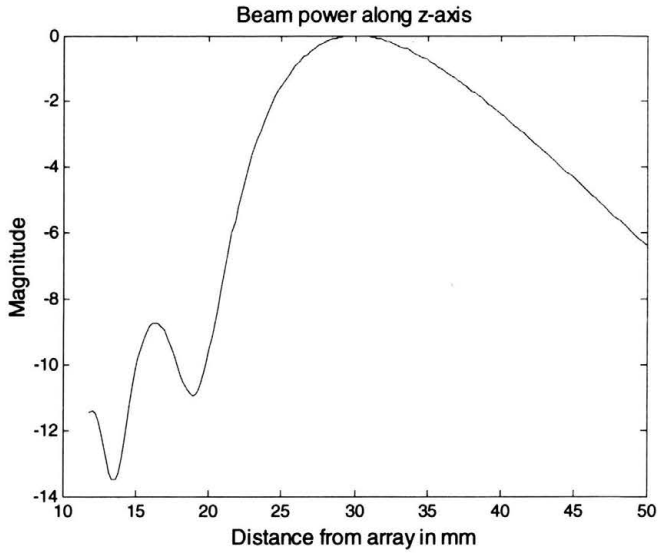

FIGURE 7. Beam power along the axis z for the array shown in Fig. 5.

4.1. Spatial aliasing

Consider the unsteered beam with beam pattern defined by Eq. (3.2), it can be proven [1, 3] that the magnitude of the beam pattern is given by

$$|b(\omega,\psi)| = \left|\frac{\sin(\pi\delta M \sin\psi)}{\sin(\pi\delta \sin\psi)}\right|, \quad \text{where} \quad \delta = \frac{df}{c}. \tag{4.2}$$

For far field the angle ψ is small and we can use the approximation

$$|b(\omega, \psi)| \approx \left| \frac{\sin(\pi\delta\, M\, \psi)}{\sin(\pi\delta\, \psi)} \right|. \tag{4.3}$$

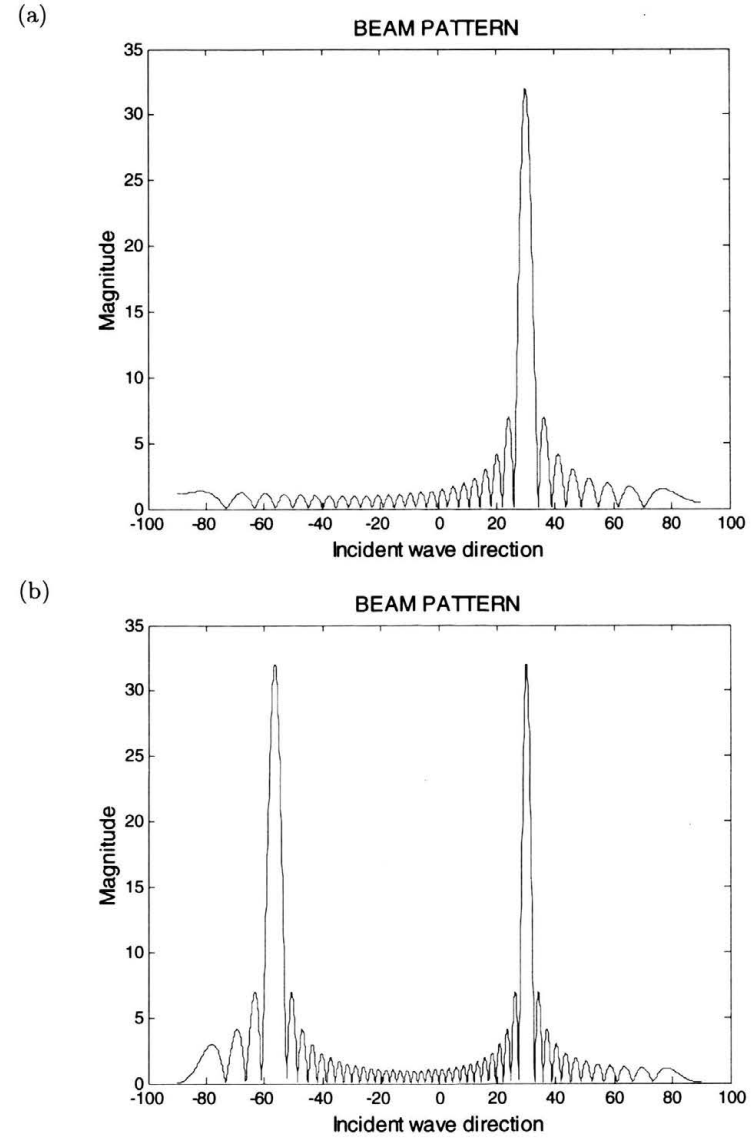

FIGURE 8. Radiation patterns for the array A32EL steered with an angle 30° without apodization for spacing $d = 0.5\lambda$ (a) and $d = 0.75\lambda$ (b).

Thus, Eq. (4.3) attains a maximum when the denominator is zero, that is for

$$\pi\delta\,\psi = n\pi \quad \text{for} \quad n = 0, \pm 1, \pm 2, \Lambda.$$

This means that the beam pattern is periodic, since it has its maximum not only for $\psi = 0$ but also repeating peaks at $\psi = n/\delta$. The repeating peaks define so-called *grating lobes* that appear due to the discrete nature of the array. This undesirable effect is known as *spatial aliasing*. Position of the grating lobes in space is defined by the relative separation δ, that is, for a wave with frequency f propagating in a medium characterized by the sound velocity c the array spacing d can be used to control position of the grating lobes.

Consider $\delta = 1/2$, that is the array spacing equal to half wavelength, $d = \lambda/2$, then the first grating lobes will appear at $\pm 90°$ which is also the maximum steering angle possible. The array separation $d = \lambda/2$ eliminates spatial aliasing and corresponds to the *Nyquist frequency* in signal processing [1, 2]. Spatial aliasing should be taken into account during array design, especially when the array is to be steered with larger angles (see Fig. 8 illustrating aliasing problem). From Fig. 8, it can be seen that increasing array spacing above $\lambda/2$ results in a grating lobe that appears at an undesired angle. Amplitude of this lobe can be attenuated by an efficient apodization.

4.2. Spatial resolution

Spatial resolution of an array is determined by the width of its main lobe given an accepted level of side lobes. Consider Eq. (4.3), for small values of ψ it can be approximated by

$$|b(\omega, \psi)| \approx \left| \frac{\sin(\pi\delta\, M\, \psi)}{\pi\delta\,\psi} \right|, \tag{4.4}$$

which is known as the *sine* function of peak value M.

The *3dB (half power) beam width* defines an angle Θ_{3dB} that is used as a measure of spatial resolution as

$$\theta_{3dB} = 0.89\ \arcsin(M\delta)^{-1} = 0.89\ \arcsin\left(\frac{\lambda}{Md}\right). \tag{4.5}$$

Thus, the spatial resolution of an array is inverse by proportional to the product of its relative separation δ and the number of its elements (cf. Fig. 9). The above definition is valid for an array without apodization only, as it was mentioned above, apodization decreases the resolution and attenuates the side lobes.

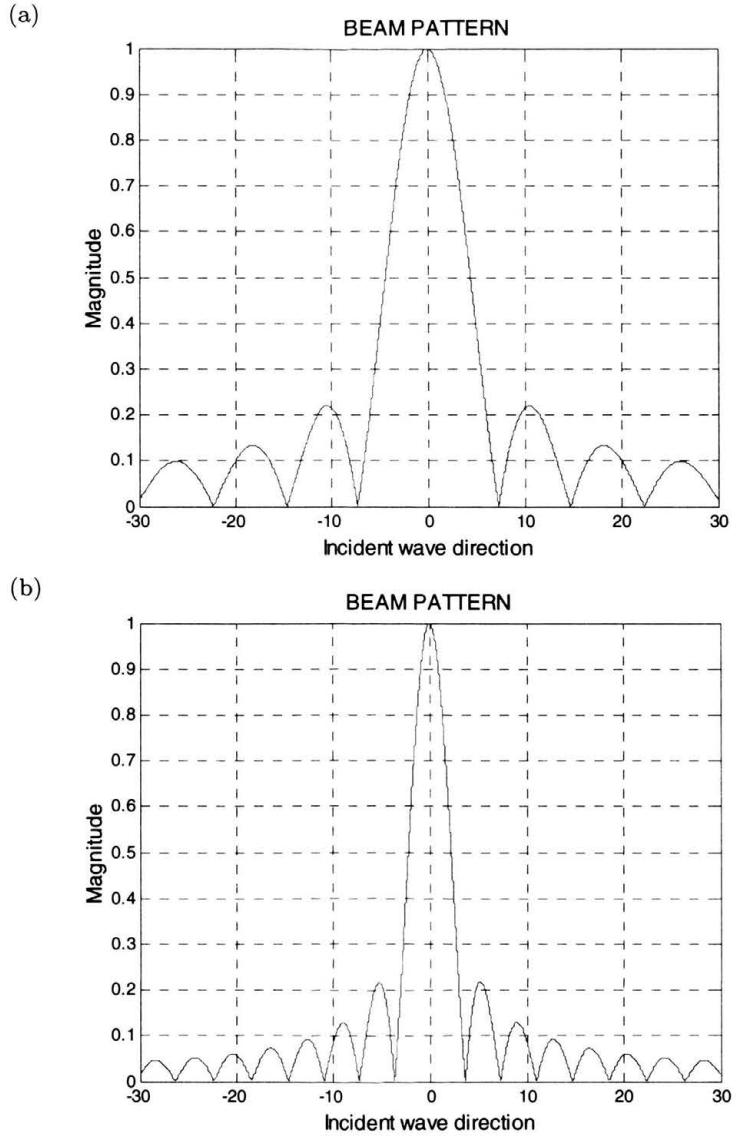

FIGURE 9. Normalized radiation patterns for the array consisting of 16 elements (a) and 32 elements (b). Element spacing $d = 0.5\lambda$, no apodization.

5. Beamformers

Beamforming in transmission is rather simple for practical realization, array elements are excited by the pulses that are generated at different time instances to form a desired wave front. However, beamforming in the recep-

tion is far more complicated since the signals received by the array elements have to be delayed to enable coherent summation according to the scheme shown in Fig. 10. The delay elements denoted by $\tau_1, \ldots, \tau_N$ delay the received signals, their amplitude is then modified by the apodization coefficients $a_1, \ldots, a_N$ and a coherent sum is produced in the end.

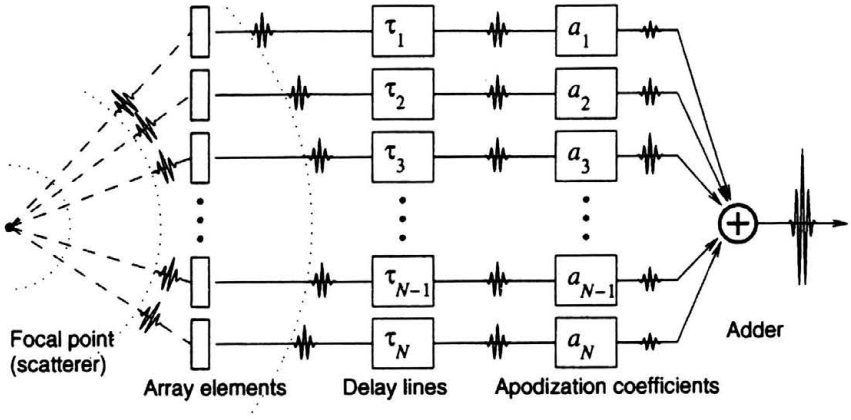

FIGURE 10. A time domain delay and sum beamformer.

Modern beamformers employ A/D converters for converting signals received by the array elements into a digital form. The A/D converters have to be characterized both by a high sampling frequency (tenths of MHz) and by high resolution (10 bits at least). In many applications low power consumption can also be an important requirement.

However, the most difficult issue is providing sufficient resolution for the discrete time delay elements (denoted by $\tau_1, \ldots, \tau_N$ in Fig. 10). Suppose that the sampling frequency f_s is 10 times higher that the transducer's center frequency, $f_s = 10f_0$. Typical transducer may have 100% bandwidth, which means it would receive signals with the highest frequency $1.5f_0$, which according to Nyquist theorem would require sampling frequency $3f_0$. Thus, from the signal processing point of view the signal would be over-sampled, however, the resolution in delay measured in degrees would be only $360°/10 = 36°$. Increasing sampling frequency is expensive and unjustified since the signal bandwidth is limited by the transducer (array).

One solution to this problem consists in using some type of *interpolation filter*, that is, an artificial technique that involves increasing the effective sampling frequency by an integer factor. This can be relatively easily done for the band-limited signals received by the array elements.

Another solution, often used in medical instruments employs *quadrature demodulation*, consisting in shifting the signal of interest to a lower frequency band, before sampling. The significant decrease in frequency obtained in this way releases sampling constraints and enables using relatively high sampling rates.

6. Applications of phased arrays in NDT

Improvement of the characteristics of 1-3 piezoelectric composite has enabled rapid development of the high performance phased-array systems for industrial applications. A piezoelectric composite is fabricated so that the tiny pillars made of piezoelectric ceramics are configured in an array, as shown in Fig. 11, and compacted into a composite by filling with resin. Then the thickness of the composite plate is adjusted according to the desired frequency and thin electrodes are manufactured on both its sides. On one side of the plate the electrodes have to be shaped in the form of array elements. The main advantages of the composite arrays are their relatively low price and low acoustic impedance that improves matching to water in the immersion inspection. They are also characterized by a low value of mechanical Q_m (Q_m is an index representing damping characteristics of piezoelectric composite) that results in the increased bandwidth and in consequence the improved temporal resolution.

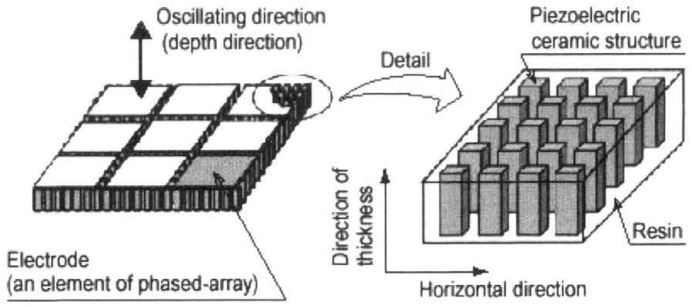

FIGURE 11. Structure of the 1-3 piezoelectric composite.

The first major application of the phased array technology in NDT is the inspection of complex geometry parts. When a conventional UT is used, the inspected volumes often have to be scanned entirely with a number of angle probes. Serious problems may be encountered when there is a limited access only to the inspected volume from the outside. Typical example is

the inspection of turbine rings and blades shown in Fig. 12. Such structures can be inspected using the beam scanning function of the phased array that replaces complex mechanical scanning using conventional probes.

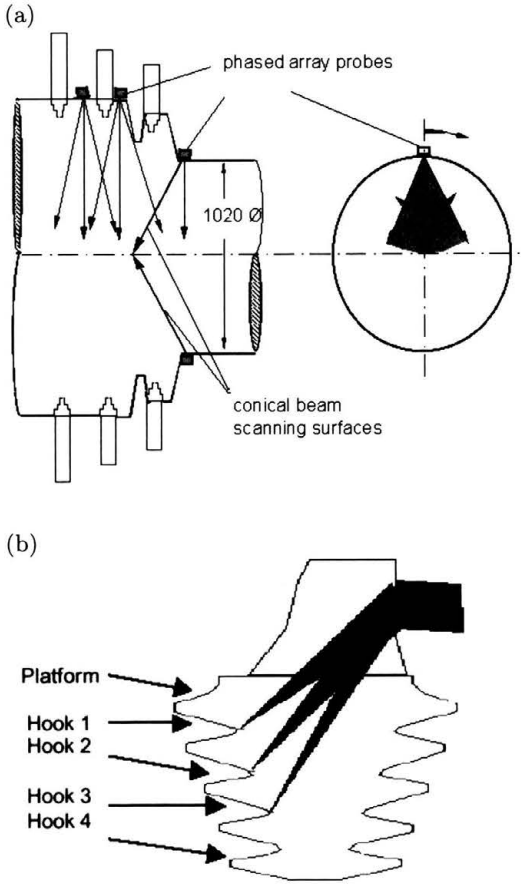

FIGURE 12. Turbine inspection using phased array. Turbine ring inspection (a) and turbine blade inspection (b).

Phased arrays are also used for the ultrasonic inspection of butt welds shown in Fig. 13. Two different principles can be used for this purpose, electronic scanning (beam multiplexing) and beam steering. Electronic scanning is performed using a group of active array elements (an aperture that can be also focused), which is shifted along the array using electronic multiplexer.

Electronic multiplexing consisting in switching each element group electrically, as illustrated in Fig. 14, eliminates mechanical scanning and considerably increases inspection speed.

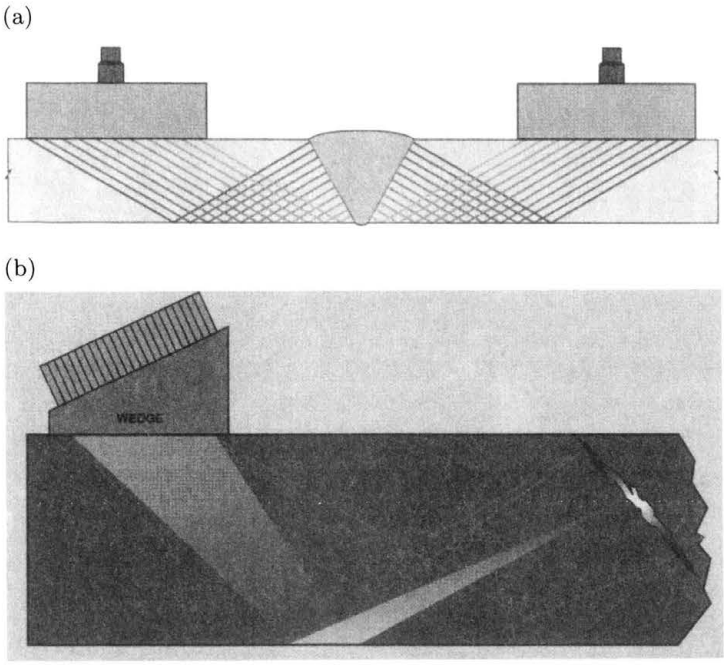

FIGURE 13. Weld inspection using phased array. Beam multiplexing (a) and beam steering and focusing (b). Courtesy of R/D Tech.

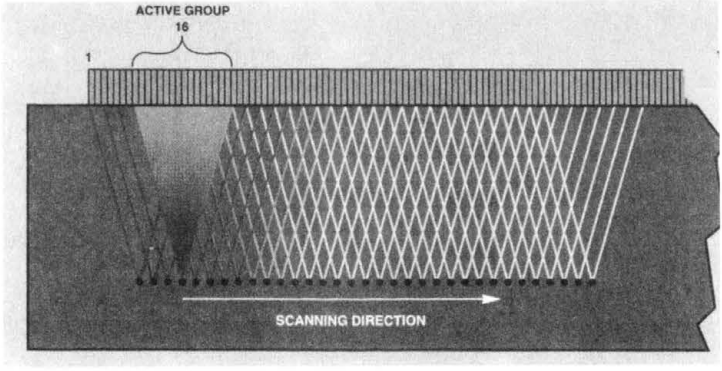

FIGURE 14. Electronic scanning using beam multiplexing. Courtesy of R/D Tech.

Electronic multiplexing can be very useful in inspection of tubular products because it is capable of replacing complex rotating ultrasonic heads. The inspection principle is illustrated in Fig. 15 where an encircling ultrasonic array is used for tube inspection. A group of elements (an active aperture)

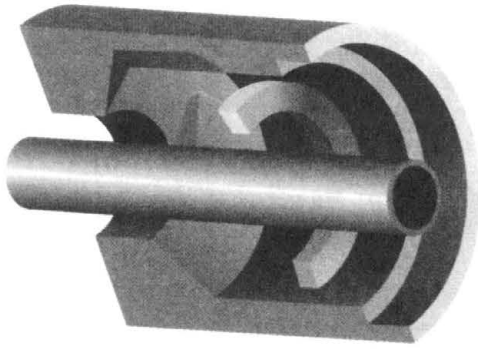

FIGURE 15. Electronic scanning used for tube inspection. A beam produced by an active aperture is reflected by a special mirror. Courtesy of R/D Tech.

is used to obtain a focused and steered beam that is reflected by a mirror to reach the inspected tube. The active aperture is multiplexed producing an artificial rotation. A number of such apertures can be used at the same time to increase the inspection speed. Separate arrays (with or without mirrors) are normally used for detecting longitudinal and transversal defects and thickness measurement.

7. Summary

This paper serves as an introduction to phased arrays based on time-domain beamforming. It starts with the presentation of beamforming fundamentals using the spatial filtering approach. This approach consist in designing the response of an array so that it becomes sensitive to signals coming from a desired direction while signals from other directions are attenuated. The theory is illustrated by a number of beamforming examples simulated using MATLAB.

Issues related to the design of a time domain beam former hardware are shortly reviewed.

Finally, practical applications of phased arrays to the inspection of turbines, butt welds, and tubular products are presented.

References

1. G.S. KINO, *Acoustic Waves: Devices, Imaging and Analog Signal Processing*, Prentice-Hall, Inc., 1987.

2. M. SOUMEKH, *Synthetic Aperture Radar Signal Processing*, John Wiley 6 Sons, Inc., 1999.

3. J. GOODMAN, *Introduction to Fourier Optics* (2nd edition), MacGraw-Hill, 1996.

4. B.D. VAN VEEN, K.M. BUCKLEY, Beamforming: A versatile approach to spatial filtering, *IEEE ASSP Magazine*, April, 1988.

5. P. MCINTIRE (Ed.), *Nondestructive Testing Handbook*, Vol.Seven, Ultrasonic Testing, Section 9, Multiple Transducer Ultrasonic Techniques, (2nd edition), ASNT, 1991.

6. S.R. GHORAYEB, W. LORD, S.S. UDPA, Application of beamforming technique to ultrasound imaging in nondestructive testing, *IEEE Trans. On Ultrasonics, Ferroelectrics and Frequency Control*, Vol.41, March 1994, pp.199-208.

7. W.G. GEBHARDT, *Electronic Beam Forming, Defect Reconstruction and Classification by Ultrasonic Phased Arrays, in Nondestructive Testing*, edited by R.S. Sharpe, Vol.7, Academic Press, 1984.